Proc. Indian Acad. Sci. (Chem. Sci.), Vol. 93, No. 3, April 1984, pp. 389–406.

Glass transition. A new approach based on cluster model of glasses*

K J RAO

Solid State and Structural Chemistry unit, Indian Institute of Science, Bangalore 560012, India

Abstract. The structure of real glasses has been considered to be microheterogeneous, composed of clusters and connective tissue. Particles in the cluster are assumed to be highly correlated in positions. The tissue is considered to have a truly amorphous structure with its particles vibrating in highly anharmonic potentials. Glass transition is recognized as corresponding to the melting of clusters. A simple mathematical model has been developed which accounts for various known features associated with glass transition, such as range of glass transition temperature, T_g, variation of T_g with pressure, etc. Expressions for configurational thermodynamic properties and transport properties of glass forming systems are derived from the model. The relevence and limitations of the model are also discussed.

Keywords. Glass transitions; cluster model; thermodynamic properties; transport properties.

1. Introduction

Glass transition continues to be an enigmatic feature of glassy state. Several attempts have been made in the literature to model the transition theoretically and all such efforts have succeeded only partially. A more recent observation of significance in this context is that most real glasses are microheterogeneous in structure as evidenced from a number of sophisticated experiments. Hence, the limitations suffered by earlier glass transition models may atleast be partly attributed to the assumption of a homogeneous random structure of glasses implied in them. In this work, an attempt has been made to understand glass transition giving specific recognition to the microheterogeneous nature of the glasses. A few experimental aspects related to glassy state and glass transition are summarized in §2. Salient features of earlier glass transition theories are summarized in §3. Evidences that support microheterogeneous structure of glasses are briefly referred to in §4, and a simple mathematical model of glass transition based on cluster concept is developed in §5, where in model results are also discussed. In succeeding sections, the thermodynamic and transport properties derived from the model are presented and the possible limitations of the model are discussed in the concluding section.

2. Glass formation and features of glass transition

Glass is the resultant solid product when a melt is cooled in such a way that crystallization is bypassed (Turnbull 1969). Rates of cooling required for the formation of glasses, however, vary widely. For example it is of the order of million degrees/sec for cooling metallic melts into the glasses while it is a negligible fraction of degree/sec for

* Contribution No. 251 from Solid State and Structural Chemistry Unit.

cooling B_2O_3 melt into glass (Owen 1973). In the temperature region below the melting point (liquidus temperature) volume and entropy of the super cooled liquid decrease continuously into the glassy state (figure 1a). But the slopes of their variations exhibit changes over a narrow region of temperature prior to solidification. This effect is even more clearly evident in heat capacity and thermal expansivity plots where 'more or less' sudden changes occur in a narrow region of temperature (Rao 1979). The phenomenon is referred to as glass transition. The glass transition is generally reversible. An operationally-defined glass transition temperature, T_g, refers to the intersection of linear extrapolations of heat capacity curves as shown in figure 1b.

The region between T_g and T_m is referred to as supercooled liquid. The experimental glass transition temperature is a function of the cooling rate and is higher for higher cooling rates. Heat capacity plots almost universally exhibit a hump on the heating cycle. The magnitude of the hump increases for well-annealed glasses (Moynihan *et al* 1976).

Viscosity (and other transport properties) varies exponentially in the supercooled region and as the glass transition is approached viscosity attains a value of $\sim 10^{13}$ poises. It may be easily recognized that such high viscosities correspond to characteristic relaxation times of the order of minutes and it far exceeds laboratory time scales for general physical property measurements. Hence the supercooled liquid manifests as a solid capable of sustaining normal shear forces and with characteristic solid like heat capacity. The variation of viscosity in the supercooled region often exhibits a non-Arrhenius behaviour in many glass-forming melts (Angell and Moynihan 1969)

$$\eta = \eta_0 \exp\left[E_\eta/(T-T_\eta)\right], \tag{1}$$

where η_0, E_η and T_η are constants of the Vogel-Tamman-Fulcher equation for viscosity. T_η which has units of temperature renders the viscosity formally infinite when the temperature of measurement is equal to it and indeed suggests a rheological limit to the liquid regime. This parameter not only linearizes the otherwise nonlinear η vs $(1/T)$ plots (where $\ln \eta$ is plotted as function of $[1/(T-T_\eta)]$) but is numerically always

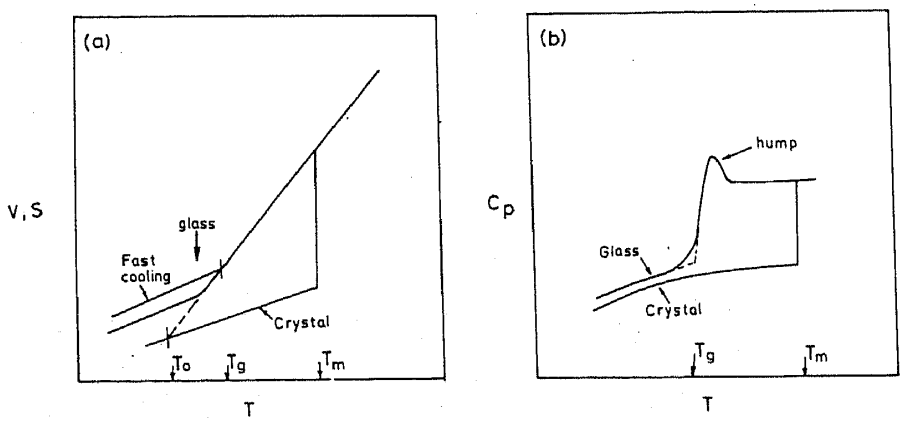

Figure 1. Schematic of variation of thermodynamic properties during glass transition: (**a**) Volume (V) and entropy (S) variation with temperature. Lower T_g corresponds to slower cooling rates. T_0 is the thermodynamic limit to glass transition temperature indicated by extrapolation of entropy lines. T_m is the melting point of the crystalline material of same chemical composition. (**b**) Variation of heat capacity with temperature. T_g is indicated as intersection of extrapolated lines. Note the hump in C_p variation.

lower than the experimental T_g. No instance is known where T_η is greater than T_g. The magnitude of $(T_g - T_\eta)$ decreases as the glasses are annealed.

The entropy plot in figure 1a is also quite revealing. While slower and slower cooling rates bring glass entropy closer and closer to the entropy of parent crystalline phase the entropy lines are never known to cross each other. Indeed if intersection occurs an apparent violation of the third law of thermodynamics would ensue, since the supercooled liquid which is inherently disordered would have a lower entropy than the corresponding ordered crystalline state (Kauzmann 1948) (Kauzmann paradox). Intersection of the extrapolated entropy line of the supercooled liquid with that of the crystalline solid corresponds to a zero configurational entropy state and can be estimated (normally done through the so-called Kauzmann plots, where heat capacity is plotted as a function of ln T and the area matching is utilized to determine the isentropic amorphous state) (Angell and Rao 1972). Such a temperature is referred to as T_0 which may be considered as a thermodynamic limit to disordered liquid state. Below this temperature the transformed amorphous solid possesses zero configurational entropy or (as Kauzmann suggested) the material may undergo a transition to an ordered crystalline solid. While it is interesting to note that T_0 and T_η both suggest a certain temperature limit to the liquid state from thermodynamic and kinetic points of view respectively, it is intriguing that $T_\eta = T_0$ within experimental limits of accuracy in well-documented systems in literature (Angell and Moynihan 1969).

We may therefore infer that infinitely slow cooling of a melt, would result in an equilibrium transition to a glass at a temperature, $T = T_0 = T_\eta$. Unattainability of infinitely slow cooling rates, however, causes the supercooled melt to fall out of the equilibrium at $T_g > T_0$ in an experimental glass transition. Such arguments suggest that an equilibrium thermodynamic transition is latent and that it does not manifest due to kinetic reasons. The thermodynamic nature of such a glass transition is also suggested by the fact that T_g/T_m (T_m is the melting or liquidus temperature) is $\sim$ 2/3 for a large variety of glasses (Sakka and MacKenzie 1971). A real glass therefore possesses a frozen entropy, a measure of which is indicated in the Kauzmann plot in figure 2. The frozen entropy is large in covalently-bonded oxide glass systems as compared to ionic glass

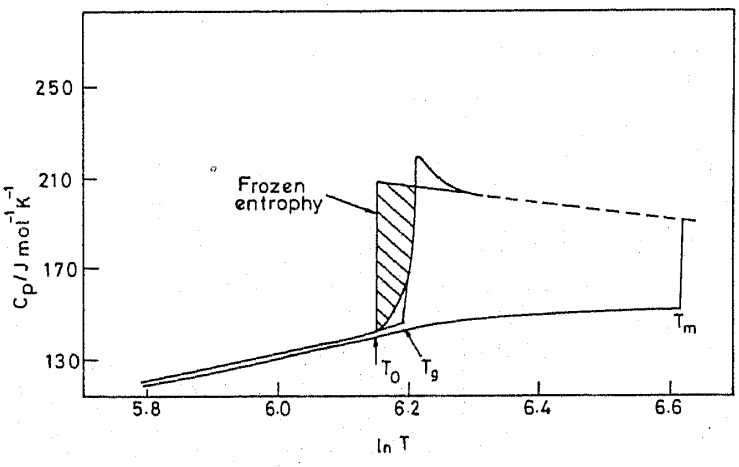

Figure 2. Typical Kauzmann plot obtained from heat capacity measurements (C_p vs ln$T$ data on a sulphate glass from author's laboratory). Frozen entropy is shown by hatching the area.

systems such as those of nitrates and sulphates. The discontinuity in the heat capacities at the glass transition, ΔC_p is also recognized as a characteristic parameter of the glasses and it is generally larger in ionic glasses than in covalently bonded oxide glasses (Angell and Sichina 1976).

3. Theories of glass transition

Many modelistic approaches have been made in literature (Rao 1979; Parthasarathy *et al* 1984) in order to understand the various features of glass transition which were briefly described in the preceding paragraphs. Among them the free volume theory (Cohen and Turnbull 1959; Turnbull and Cohen 1961, 1970) has laid emphasis on concomitant decreases in volume and fluidity of glass-forming melts in the supercooled region. Therefore glass transition has been related to the decrease of free volume associated with particles. Below a critical value of free volume particle transport is considered impossible. A recent extension of free volume model (Cohen and Grest 1980, 1981) in conjunction with percolation concepts has imputed a first order character to glass transition at $T < T_g$.

A thermodynamic theory for glass transition was developed by Gibbs and coworkers (Gibbs and DiMarzio 1958; Adam and Gibbs 1965; Gibbs 1963) wherein the configurational entropy was related to the viscosity. The primary transport event was associated with the plurality of attainable particle configurations. The experimental T_g in this theory is directly related to the falling out of equilibrium of the system at low values of configurational entropy, because attainment of different configurational states requires a high degree of cooperativity. Also, entropy theory directly implies a zero-configurational entropy ground state of amorphous materials. In another approach to glass transition Goldstein (1969, 1976a, 1977) has suggested that the configurational state of a supercooled liquid, can be described through a energy hypersurface of position and momentum coordinates and that the glass transition occurs when the system of particles gets trapped upon cooling into one of the many potential minima which are present on such a hypersurface. All such theoretical approaches attempt to describe the thermal variation of a suitable liquid property such as volume, entropy or enthalpy and seek to identify the glass transition as a terminal event in the behaviour of a supercooled liquid. Several well-known limitations of these approaches have been discussed elsewhere (Rao 1979; Parthasarathy *et al* 1984; Goldstein 1963, 1976b).

In a basically different approach Angell and Rao (Rao and Angell 1971; Angell and Rao 1972) sought to discuss glass transition using concepts of Ising model developed for crystalline phase transitions. They abstracted a lattice of bonds from the non-periodic glass structure and considered the consequences of excitation of bonds. An appropriate concentration of such broken bonds around the particle would give rise to the familiar transport. The model could account for the rapid heat capacity increases, a characteristic of glass transition but suggests that no discontinuities of C_p may occur at T_g. Other limitations of this model are discussed in literature (Goldstein 1976b; Rao 1979).

4. Intermediate range structure in glasses

The continuing efforts in modelling glass transition are a pointer to the fact that the current models of glass transition are unsatisfactory. The reason for this situation could

be that the models have ignored or failed to recognize the role of intermediate range structure in glasses and have assumed that glasses possess a completely random and homogenous structure. Many recent experimental evidences do not support this assumption (Zarzycki and Mezard 1962; Schmidt *et al* 1980; Gaskell *et al* 1979; Bursill *et al* 1981; Phillips 1982; Sundar *et al* 1982; Parthasarathy *et al* 1981; Hemlata *et al* 1983; McCall 1973; Rubinstein 1976; Hoare and Barker 1976; Hoare 1976). Foremost among such evidences are results of high resolution electron microscopy of metallic (Gaskell *et al* 1979) and ionic glasses (Bursill *et al* 1981) which indicate the presence of fringe patterns characteristic of crystalline order extending to dimensions of ~ 50 Å. Many evidences from spectroscopy reveal the existence of intermediate range order extending upto 50–100 Å in space even in SiO_2 and GeO_2 glasses and have been recently discussed by Phillips (1982). Computer experiments (Hoare and Barker 1976; Hoare 1976) also suggest the presence of large clusters called amorphons in which the particle positions are highly correlated. Amorphons are built basically with non-space filling icosahedral motifs and can be as large as several hundred atoms in size. Therefore any new approach to glass transition has to recognize the possibility of such high degree of atomic correlation over distances of the order of 50–100 Å, and its influence on the detailed atomistic processes characterizing the transition.

5. Cluster model of glasses and glass transition

The cluster model of glass recognizes the presence of intermediate range structure. In this model glass is considered to be made up of highly correlated regions known as clusters which are held together by 'connective tissue material' (Hoare and Barker 1976; Hoare 1976; Haddad and Goldstein 1978). Though not clearly stated by earlier workers it is intutively obvious that the connective tissue is characterized by a much lower degree of correlation so that it may be considered as truly amorphous. Since the origin of the tissue is that it is the 'left over' material after full development of clusters while cooling the melt, it is reasonable to assume that they have a slightly lower density than the clusters. The nature of the high degree of correlation in the cluster can be either one of microcrystallites or of large amorphons. Such a description is particularly relevent to ionic, metallic and molecular (small molecules) glasses. However in highly covalently bonded glasses like SiO_2, GeO_2, B_2O_3, As_2Se_3 etc also, clusters are formed during cooling by rebonding of molecular fragments which are present in their melts.

In the cluster model, transition of supercooled melt into a glass is visualized as follows. Supercooled region of melts is characterized by fairly large scale density and compositional fluctuations which nucleate the clusters at low enough temperatures. Such clusters grow in size rapidly but their growths become self-limiting at sizes of 50–100 Å. Glass transition occurs when a major part of the melt is thus transformed to clusters and these clusters impinge on each other; the remaining tissue material simply freezes (Rao and Rao 1982).

The reason for the self-limiting growth of amorphon-like clusters is fairly obvious, since beyond a certain size such ensembles become energetically unfavourable (Burton 1970, 1973a, b). In the case of the covalently-bonded clusters, occurrence of topological (wrong directionality of bond popagation or wrong dihedral angles) and compositional (wrong bond), disorder may act to terminate the growth (Phillips 1982). In metallic and multicomponent ionic glasses where the clusters are in many instances appear to be microcrystalline, self-limiting growth is most likely a consequence of just the

compositional disorder over microscopic scales. Since the cluster and the tissue have an interface, mobile atoms or ions in the system may be looked upon as distributed unequally in these two regions in accordance with a distribution law (equalization of chemical potentials). This composition gradient at the interface is counteracted by the tendency for randomization (entropy force) and hence growth of the clusters attains a limit. It may also be seen that such small compositional differences offset the free energy gains that would accrue from further increase of the cluster volume.

We therefore assume that a cluster-tissue scenario is quite generally applicable to all types of glasses. Thus, a microheterogenous structure is recognized here as an inherent feature of all real glasses. A simple mathematical model for glass transition is developed below for such a microheterogeneous glass. The model may be particularly relevant to ionic glasses.

Particles in a glass made up of cluster and tissue regions fall into three categories: (a) Particles inside the cluster which vibrate in essentially harmonic potentials. (b) Particles in the tissue-region which vibrate in shallow and highly anharmonic potential wells. These potential wells coalese at higher (thermally accessible) energies. (c) Particles on the cluster surface which vibrate in potential wells of substantially high degree of anharmonicity which are characterized by a slowly rising potential towards the tissue region. The effect of temperature on such a glass may be viewed as follows. The particles are vibrationally excited in all the three regions. However, the vibrational levels in the tissue region are closer and particles are easily excited into various levels. Since the higher energy levels in this region correspond to coalesced potential wells (doubly, triply etc., multiply connected), particles execute oscillations with systematically increasing amplitudes. Particles on the surface of clusters also undergo similar vibrational exitations and are driven to the multiply connected regions of potentials. Large amplitude vibrations of particles allow a permanent escape of such particles from the surface of the cluster. When particles leave the surface of a cluster in this manner a new set of surface particles are exposed from the interior of the cluster. Also the total number of particles in the tissue region increases. Therefore as the temperature increases not only the population in the higher vibrational energy levels increases but the total number of particles in the tissue region also increases at the expense of clusters whose sizes keep shrinking. The process continues till clusters shrink and shed all particles into the tissue region. The temperature at which clusters vanish corresponds to the glass transition temperature T_g^0, in this model. We may therefore note that the presence of such multiply connected wells allows for a gradual evolution of translatory motion from a vibratory motion. Further, to a first approximation, excitations into the vibrational energy spectrum of tissue region may be considered as sufficient for discussion of configurational properties associated with glass transition.

Since the cluster surfaces act as a source of particles for the tissue during heating and these particles are distributed into the spectrum of energy levels, we may note that there is a quasiequilibrium of particles on the surface and particles in the spectrum of energy levels.

$$\text{Particles on cluster surfaces} \rightleftharpoons \text{Particles in the vibrational energy manifold} \tag{2}$$

5.1 *Formulation of the model*

The problem of glass transition, therefore, reduces to finding out how the sizes of

clusters decrease as a function of temperature. This rate is related to the rate at which the surface particles 'melt' into the tissue which in turn is related to the rate at which the tissue particles near the cluster surface diffuse away. Since diffusive step occurs through the excitation of particles into multiply-connected higher energy levels in the tissue region, the rate of dissolution depends on the rate at which the higher energy levels are populated. The cluster particles may jump into the vibrational manifold of the tissue at any energy level depending on the structure of potential wells. However, since the particles in the tissue as a whole re-establish an equilibrium distribution in accordance with an appropriate partition function the quasi equilibrium in relation (2) is valid. If the number of vibrational states we wish to consider is sufficiently large and if the temperature is not very high in comparison with energy separation of ground and first-excited states, the ground state is always the most populated. In view of these considerations we assume that till clusters melt fully (upto T_g^0) the number of particles in the ground vibrational state remains constant.

Let f_0 represent the fraction of particles in the ground vibrational state of tissue region at a temperature T. If N_t is the number of particles in the tissue region, then

$$N_t f_0 = \text{constant.}$$

Therefore,

$$\mathrm{d}(N_t f_0)/\mathrm{d}T = 0,$$

or

$$\mathrm{d}\ln N_t/\mathrm{d}T = -\mathrm{d}\ln f_0/\mathrm{d}T. \tag{3}$$

Let V_c and V_t be the volumes of clusters and tissue so that the total volume V is

$$V = V_c + V_t = \text{constant.}$$

If N_0 is the number density of particles (approximately equal for both tissue and cluster regions), we have

$$V_c + (N_t/N_0) = \text{constant},$$

or

$$\mathrm{d}V_c/\mathrm{d}T = -V_t\frac{\mathrm{d}\ln N_t}{\mathrm{d}T} = -(V-V_c)\frac{\mathrm{d}\ln N_t}{\mathrm{d}T}. \tag{4}$$

Therefore, from (2) and (4),

$$\frac{1}{(V-V_c)}\frac{\mathrm{d}V_c}{\mathrm{d}T} = \frac{\mathrm{d}\ln f_0}{\mathrm{d}T}. \tag{5}$$

Integrating both sides with respect to temperature

$$\int_{T=0}^{T}\frac{\mathrm{d}V_c}{V-V_c} = \int_{T=0}^{T}\mathrm{d}\ln f_0. \tag{6}$$

Since $\ln f_0$ at 0 K is zero we can write,

$$\ln[(V-V_c^0)/(V-V_c^T)] = \ln f_0(T), \tag{7}$$

where V_c^0 and V_c^T are cluster volumes at temperatures 0 and T (deg K) respectively and $f_0(T)$ is the fractional population in the ground vibrational state at T. Let us suppose that the total volume of glass and volume of clusters at 0 K are related as $V = aV_c^0$,

where a is a constant (somewhat affected by the thermal history of the glass). Equation (7) may be written as

$$\ln[(a-1)/a] - \ln[1-(V_c^T/aV_c^0)] = \ln f_0(T),$$

or

$$V_c^T/V_c^0 = a\left[1 - \frac{(a-1)}{a}\frac{1}{f_0(T)}\right]. \tag{8}$$

We may recognize that if we used a simple form of partition function,

$$Z = \sum_{i=0}^{n} \exp[-\varepsilon_i/RT], \tag{9}$$

with $\varepsilon_0 = 0$, we have $f_0(T) = 1/Z$, so that

$$V_c^T/V_c^0 = a\left(1 - \frac{(a-1)}{a}Z\right). \tag{10}$$

Equation (10) implies that (V_c^T/V_c^0) decreases from unity to zero as T increases from 0 to T_g^0, the glass transition temperature. Since V_c is total cluster volume, $V_c = \Sigma v_{ci}$ where v_{ci}, is the volume of the ith cluster. If we further assume that cluster volumes have a narrow distribution, then $V_c = n\langle v_{ci}\rangle$ where $\langle v_{ci}\rangle$ is the average cluster volume and n is the total number of clusters. One can then define $\bar{r}_c = \langle v_{ci}\rangle^{1/3}$ as an average linear dimension of the cluster. Since clusters possess a high degree of positional correlation or microcrystalline order, $\bar{r}_c$ may be looked upon as average propagation length of a phonon mode. Hence $(\bar{r}_c^T/\bar{r}_c^0) = [\langle v_c^T\rangle/\langle v_c^0\rangle]^{1/3} = \xi$ may be considered as an order parameter with comprehensible significance in the cluster model. When clusters are all spherical and are of equal size, $\bar{r}_c$ corresponds to the radius of the cluster. Equation (10) becomes,

$$\xi = a^{1/3}\left(1 - \frac{(a-1)}{a}Z\right)^{1/3}. \tag{11}$$

5.2 *Evaluation of* ξ

In order to be able to investigate the behaviour of ξ as a function of temperature the energy spectrum needed to evaluate Z has to be specified and a reasonable value of a must be assigned. For a collection of spherical clusters of equal radii touching each other, $V/V_c^0 = a \sim 1{\cdot}6$, a value consistent with random close packing of clusters. No unique representation of connected potential wells can however be prescribed. A plausible schematic is shown in figure 3 for which justification lies in the nature of sensible conclusions it leads to. It represents a systematic one-at-a-time increase in the degree of coalescence of potential wells. Also every higher excited level is shown as pertaining to next coalesced stage of potential wells. The various levels and energy differences are designated so that the subscript n in ΔE_n denotes energy level separation in n-connected potential wells. The dotted lines represent 'effective' or pseudo-single potential well equivalents of the coalesced wells. If $k_1, k_2, \ldots k_n$ represent the force constants characterizing these pseudo single wells, one can write

$$\Delta E_1 = (k_1/\mu)^{1/2}; \ldots \Delta E_n = (k_n/\mu)^{1/2}, \tag{12}$$

where μ is the appropriate reduced mass. One can also approximate the amplitudes of

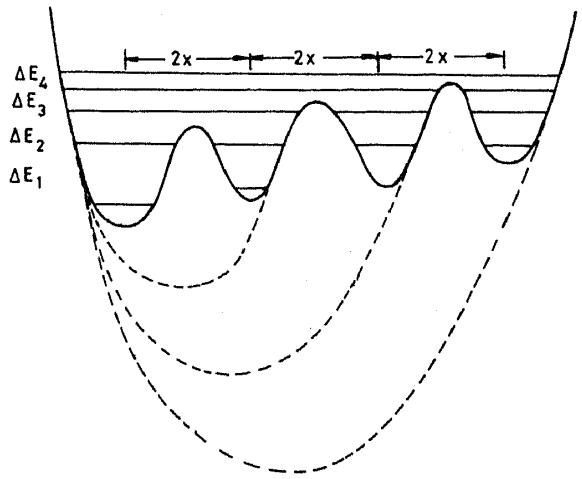

Figure 3. Schematic of vibrational energy spectrum in tissue region. ΔE_1, ΔE_2 etc are the energy separations in single and multiply connected or coalesced potential wells. The amplitudes are assumed to be $2nx$ for n-connected wells (see text).

vibration in the various pseudo wells *e.g.* $4x$ (2-connected) . . $2nx$ (n-connected) wells, where $2x$ is the assumed amplitude of vibration in single well. The vibrational potential, for example, with respect to single and two-connected wells may be equated as

$$V = \tfrac{1}{2}k_1x^2 - \tfrac{1}{3}k_1c_1x^3 = \tfrac{1}{2}k_2(2x)^2 - \tfrac{1}{3}k_2c_2(2x)^3, \tag{13}$$

where c_1 and c_2 are used as anharmonicity parameters which are small in comparison to k_1x or k_2x. Thus, (13) leads to

$$\frac{k_1}{k_2} \simeq \frac{x^2}{(2x)^2} = \frac{1}{4} = \frac{1}{2^2}.$$

Similarly for an n-connected well,

$$k_n/k_1 \simeq 1/n^2. \tag{14}$$

In view of relation (12) we have

$$\Delta E_n/\Delta E_1 = (k_n/k_1)^{1/2} = 1/n. \tag{15}$$

In other words, energy separations in an n-connected well is $(1/n)$ times the energy separation in the single well. We are now in a position to evaluate the partition function, Z, of (9) because

$$\varepsilon_n = l_1\Delta E_1 + l_2\Delta E_2 + \ldots l_n\Delta E_n,$$

where ε_n is reckoned from the ground state of single (uncoalesced) potential well and $l_1, l_2 \ldots l_n$ are the numbers of levels existing in various 'connected' wells (for the example in figure 3, $l_1 = l_2 = \ldots = 1$). Using the approximate relation of (15),

$$\varepsilon_n = \Delta E_1[l_1 + l_2/2 + l_3/3 + \ldots l_n/n]. \tag{16}$$

For the special case of figure 3

$$\varepsilon_n = \Delta E_1 \sum_{k=1}^{n} 1/k.$$

We have used the normalized energy $\Delta E_1/RT$ in the partition function and evaluated ξ

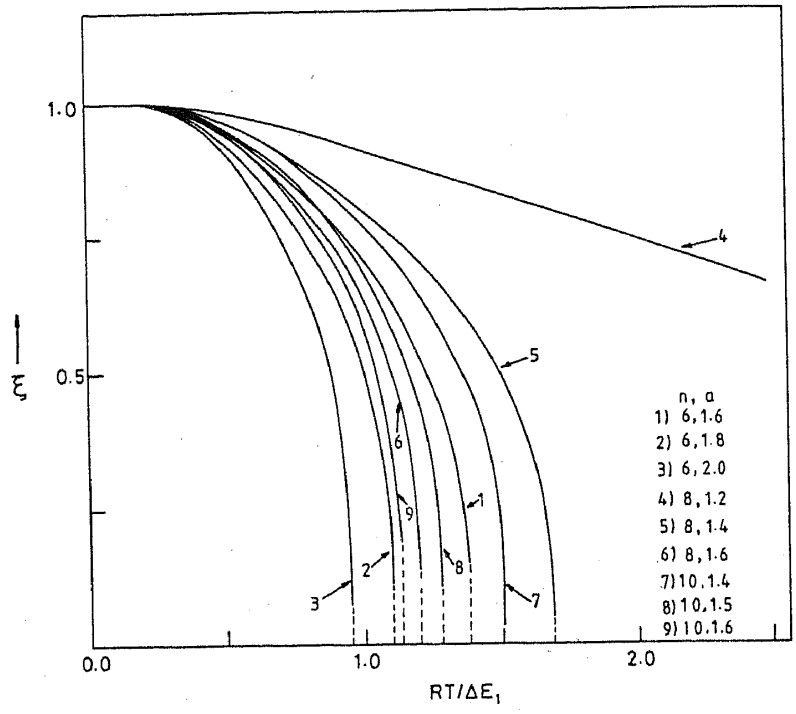

Figure 4. Variation of ξ in model calculations as a function of $RT/\Delta E_1$ for various sets of n and a values. Dotted portions indicate 'steep' fall of ξ to zero.

with a few selected values of a and n. The behaviour of ξ is shown in figure 4 as a function of the inverse of normalized energy.

5.3 *Variation of ξ and Landau theory of phase transition*

The nature of variation of ξ in figure 4 is remarkable for it is highly reminescent of the variation of order parameter in cooperative phase transitions. ξ decreases very rapidly towards higher values of $(RT/\Delta E_1)$ and $\xi \to 0$ as $T \to T_g^0$. Therefore it further strengthens the case for considering ξ as an order parameter for glass transition. The free energy density of the glass may then be expanded in terms of ξ in the neighbourhood of T_g^0;

$$\Phi(P,T,\xi) = \Phi(P,T) + b\xi^2 + d\xi^4 + \ldots \tag{17}$$

This has the immediate result that b changes sign through T_g^0 and $b = B(T - T_g^0)$. Also, the change in C_p at T_g^0 is given by

$$\Delta C_p = \frac{B^2}{2d} T_g^0. \tag{18}$$

Further

$$\xi = B^{1/2}(T - T_g^0)^{1/2}. \tag{19}$$

(Equations (18) and (19) are standard results of a Landau treatment of free energy in (17) (Rao and Rao 1979)). The exponent of $(T - T_g^0)$ in (19) suggests that this approach is in the nature of a meanfield approximation for glass transition. This supports the view that glass transition has second-order characteristics, a feature emerging from a simple consideration of Kauzmann plots of experimental heat capacity data.

5.4 *Behaviour of ξ and a in relation to T_g^0*

It is however interesting that steep changes in ξ occur towards T_g^0 which is marked by dotted lines in figure 4. If we consider this as a consequence of spontaneous dissolution of clusters whose sizes have decreased to less than some 'critical' nuclear sizes, then towards the completion of glass transition, the nature of the transition may exhibit first-order characteristics. Recently it has been suggested by Cohen and Grest (1980) that glass transition could be a first order transition. The rather large C_p humps experimentally observed by Boehm *et al* (1981) in some well-annealed fast ion conducting glasses suggest such a possibility (authors have however interpreted this as annealing effect). If indeed the dotted portions correspond to spontaneous dissolution of critical-sized nuclei whose sizes are generally 5–10 Å in radius (Kingery *et al* 1976) we would expect the radii of clusters to be of the order of 25–50 Å at 0 K which is remarkable agreement with available high resolution electron microscopic data (Gaskell *et al* 1979; Bursill *et al* 1981).

In figure 4 curves with large n correspond to large degree of coalescence and correspond to low values of T_g^0, for same value of ΔE. For higher values of a also, $\xi \to 0$ at lower values of $RT/\Delta E$. Since a is a measure of the proportion of connective tissue, increase of a amounts to increasing more open (less dense) disordered regions. Therefore ΔE itself decreases (shallower potentials). But, increase of a also implies that more states (larger n) are likely to be active (populated) in determining Z so that it reduces T_g^0. Hence the net influence of a on T_g^0 is far less obvious in the model. However, $a = 1$ corresponds to a state of zero tissue material. If an ideal glass is defined by $a = 1$, and if clusters are microcrystalline, the state of the ideal glass would be one of extremely fine-grained crystal which would only exhibit a normal melting transition. This is consistent with the value of $\varepsilon_n = l_1 \Delta E_1 + \ldots$ being very high so that $\xi \to 0$ only at very large values of $(RT/\Delta E_1)$. This conclusion is somewhat similar to early views of Kauzmann (1948). When the cluster is an 'amorphon', $a = 1$ is disallowed because the essentially spherical geometry of an amorphon becomes an overriding criterion and connective tissue is essential for the glass structure.

Glass transition temperatues can be estimated from the model. Consider a values ranging from 1·4–1·7 and $n = 4$–10. ξ becomes zero for $RT_g/\Delta E$ values between 1·2 and 2·2. For a $\Delta E \simeq 1$ kcal it would mean that T_g^0 is between 600 and 1100 K. Vibrational excitation energy of 1 kcal (400 cm^{-1}) corresponds to the cage-vibrational frequency of Li^+ ions in most Li^+ containing glasses. Also the transport properties Li^+ containing glasses are largely determined by the motion of Li^+ ions. T_g^0 of 600–1100 K estimated from the model for such glasses is therefore quite consistent with known (Button *et al* 1982; Branda *et al* 1983) T_g data. Similarly in K^+ ion containing glasses such as $Ca(NO_3)_2$–KNO_3 glasses the frequency of K^+ ion vibrations of ~ 200 cm^{-1} require T_g to be between 300 and 550 K. Indeed these glasses have typical T_g values (Rao *et al* 1973) of 330–400 K. (The choice of vibrational frequency for prediction of the glass transition temperatures of a multicomponent ionic glass is, however, an educated guess). The model also accounts for the generally low glass transition temperatures of ionic glasses. One of the predictions of this model is related to the maximum possible T_g^0 of an ionic glass. Since the highest known cage vibration frequency corresponds to that of the lightest Li^+ ion which is ~ 450 cm^{-1} and since the highest (reasonable) $RT_g/\Delta E$ at $\xi = 0$ is $\sim 2{\cdot}2$, the highest T_g^0 for a simple ionic glass is ~ 1100 K. (Though Be^{2+} should have higher vibrational frequency the only known simple glass of beryllium salt is that

of BeF_2 which is rather covalently bonded). Further the model accounts for the observed trends in many related glass systems. For example for same value of $KT_g^0/\Delta E$, T_g^0 should be lower for lower values of ΔE. This has been noticed in Li^+, Na^+, K^+, Rb^+, Cs^+ phosphate glasses in the studies of Exarhos and coworkers (Exarhos and Risen 1971; Exarhos *et al* 1974). T_g of these glasses as $(1/\mu)^{1/2}$ or as ΔE of alkali ion vibration.

In covalently-bonded glasses where molecular fragments are involved in flow process the choice of model parameters becomes rather unsatisfactory in this model.

The parameter a in the model plays important role in many experimental aspects of glass transition. In 'good' glasses, annealing may alter the value of a to some stable value which is higher than initial a. Density, refraction etc exhibit relaxations which in this model are primarily time variations of a in the annealing region. It is also to be expected that a and the conventional Toole temperature are related.

6. Thermodynamic properties from the model

Heat capacity variation around T_g which is a hallmark of glass transition may be evaluated from the model as follows. We confine ourselves to the configurational heat capacity of the glass, and in the present model, all configurational changes originate from tissue region. Since the effect of temperature is to excite the particles to various thermally accessible states in vibrational spectrum, the total heat absorbed ΔH is given by

$$\Delta H = [\Sigma \Delta E_n f_n](V_t/V), \tag{20}$$

where (V_t/V) is the fraction of the tissue material. All the quantities in (20) are already defined. Configurational heat capacity, C_p (conf) may be obtained from ΔH as,

$$C_p(\text{conf}) = (\partial \Delta H/\partial T)_p = \left(\Sigma \Delta E_n \frac{df_n}{dT}\right)\frac{V_t}{V} + (\Sigma E_n f_n)\cdot\frac{1}{V}\frac{dV_t}{dT}. \tag{21}$$

Since

$$(V_t/V) = 1 - \frac{V_c}{V_c^0}\cdot\frac{V_c^0}{V}, \frac{V_c}{V_c^0} = a\left(1 - \frac{(a-1)}{a}Z\right),$$

and $V_c^0/V = 1/a$, we may obtain all the quantities in terms of Z and a:

$$C_p(\text{conf}) = \frac{(a-1)}{a}Z\left(\sum_i \Delta E_i \frac{df_i}{dT}\right) + \left(\sum_i \Delta E_i f_i\right)(\partial Z/\partial T),$$

where the subscript i has been used in place of n to facilitate labelling double sums in later steps. Upon differentiation and some simple manipulations the above expression reduces to

$$C_p(\text{conf}) = \frac{(a-1)}{a}Z\frac{1}{RT^2}\sum_i \Delta E_i^2 f_i. \tag{22}$$

The heat capacity of the glass is given by (22) upto the glass transition temperature T_g^0, where $\xi^3 = V_c/V_c^0 = 0$ or $a = (a-1)Z$. Above T_g^0, the heat capacity is given by $(\partial \Delta H/\partial T)$ where $\Delta H = \Sigma_i \Delta E_i f_i$ and is given by

$$C_p(\text{conf}) = \frac{1}{RT^2}\left[\sum_i \Delta E_i^2 f_i - \sum_i \sum_j \Delta E_i \Delta E_j f_i f_j\right]. \tag{23}$$

An inspection of (22) and (23) suggests that while C_p rises rapidly in the transition region, at T_g^0 a sudden (step) decrease occurs because of the second term in (25). This is an inescapable feature of the model since V_t attains a maximum at T_g.

The partition function used in the above expressions is unsatisfactory for evaluating other configurational thermodynamic properties like volume thermal expansivity, α (conf) and volume compressivity β (conf). Indeed, it would be preferable to express Z using Gibbs free energies (Rice 1975; Angell and Rao 1972) rather than simple energies, so that

$$Z = 1 + \sum_i \exp(-\Delta G_i/RT), \tag{24}$$

where $\Delta G_i = \Delta E_i + P\Delta V_i - T\Delta S_i$ with ΔV_i and ΔS_i as additional molar volumes and additional vibrational entropies (as compared to ground state molar quantities) respectively. ΔV_i and ΔS_i may be assumed to be generally small so that ΔE_i is nearly equal to ΔG_i upto sufficiently high temperatures. If, however, large values of ΔV_i and ΔS_i are used one can achieve high values of C_p (conf) like in an N-state model (Angell and Rao 1972). Using the partition function in (24), (22) becomes,

$$C_p(\text{conf}) = \frac{(a-1)}{a} Z \frac{1}{RT^2} \sum_i \Delta H_i^2 f_i, \tag{25}$$

where $\Delta H_i = \Delta E_i + P\Delta V_i$. The summation in (25) implies that all excitations including those to 2-connected-3-connected etc wells, contribute to configurational heat capacity. But it is intuitively reasonable to consider that the heat absorbed in excitations to lower levels contribute to only vibrational heat capacity. Hence C_p (conf) in (25) or (27) may be computed using a reasonably high initial value of i. In figure 5 typical calculation of C_p (conf) is presented using 16 states and a $\Delta E_1 = 1$ kcal (400 cm^{-1}). In figure 5a calculated values of C_p are shown as a function of T using $i = 4$–16, $i = 6$–16 and $i = 8$–16 without entropy term (equation (23)). The behaviour of corresponding ξ is also shown in the inset. In figure 5b similar calculations are presented for the same set of a and n but with a constant ΔS_i value of 0·75 cals deg^{-1} mole^{-1}. It may be seen that the use of ΔS_i generally increases both the steepness of C_p rise and the magnitude of C_p. The magnitude of the discontinuity at the peak of the C_p curves is reduced by increasing the number of initial states ignored in computing the heat capacities. The general behaviour of C_p curves is quite comparable to experimental configurational heat capacity behaviour.

The increase in volume resulting from excitations in the tissue region, is given by

$$\Delta V = (V_t/V) \sum_i \Delta V_i \cdot f_i = \frac{(a-1)}{a} Z \sum_i \Delta V_i f_i, \tag{26}$$

α (conf) and β (conf) may be evaluated using the definitions $\alpha = 1/V(\partial V/\partial T)_p$ and $\beta = -1/V(\partial V/\partial P)_T$ along with (24) and (26). For the glassy region α(conf) and β(conf) are given by

$$\alpha(\text{conf}) = \frac{(a-1)}{a} Z \frac{1}{VRT^2} \sum_i \Delta V_i \Delta H_i f_i, \tag{27}$$

$$\beta(\text{conf}) = \frac{(a-1)}{a} Z \frac{1}{VRT} \sum_i \Delta V_i^2 f_i. \tag{28}$$

At the glass transition all the three quantities C_p (conf), α(conf) and β(conf) attain

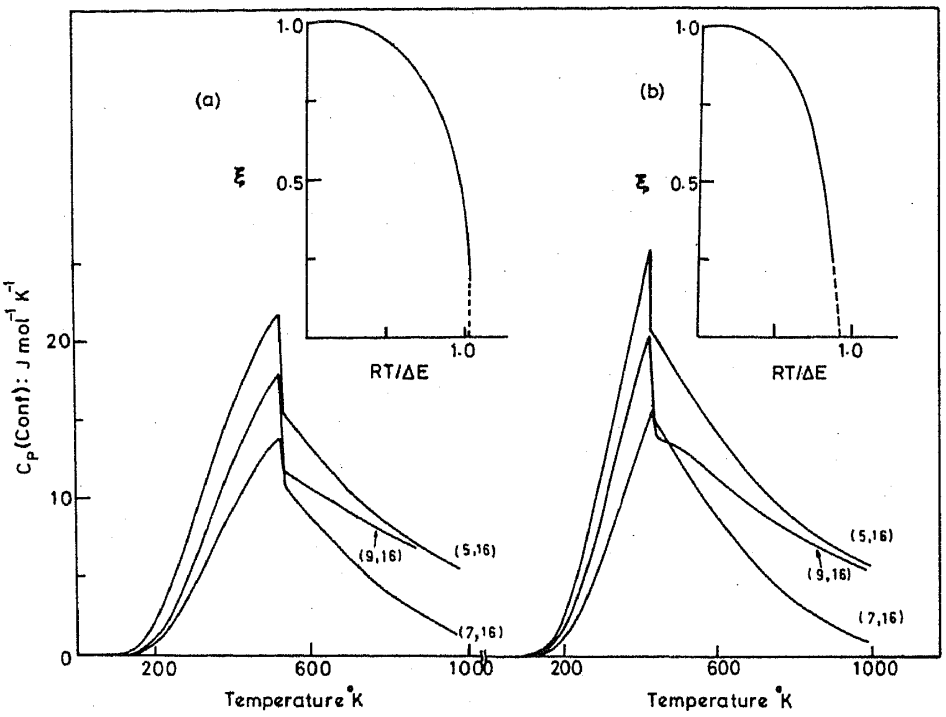

Figure 5. Heat capacity variations from the model. The numbers with in parenthesis such as (5, 16) indicate that slates $i = 5$–16 were used in computing heat capacities. Insets indicate variations of ξ for the (n, a) set employed in the C_p calculations. (**a**) and (**b**) are heat capacity variations computed without and with the use of ΔS_i. ΔS_i = constant = 0·75 cals/deg mole.

maximum values. This is because variation, $\mathrm{d}/\mathrm{d}T(V_t/V)$ is highest at T_g^0. Indeed this value may be equated to excess quantities, ΔC_p, $\Delta\alpha$ and $\Delta\beta$ usually measured at experimental T_g. We may now consider one of the relations of interest to glass transition theories, namely the Prigogine-Defay ratio, π, which is given by

$$\pi = \Delta C_p \Delta\beta / TV\Delta\alpha^2. \tag{29}$$

Since $(a-1)Z = a$ at T_g^0, (25), (27) and (28) may be combined so that

$$\pi = \frac{\left(\sum_{i=1}^{n} \Delta H_i^2 f_i\right)\cdot\left(\sum_{i=1}^{n} \Delta V_i^2 f_i\right)}{\sum_{i=1}^{n} (\Delta H_i \Delta V_i f_i)^2}. \tag{30}$$

Equation (30) may be seen to satisfy the generally known behaviour of π namely $\pi \geqslant 1$ (equality holds good when $n = 1$).

7. Effect of pressure on glass transition

The model also allows us to determine the effect of pressure on the glass transition temperature. Since at T_g^0, $\xi^3 = 0$,

$$Z = a/(a-1) = \text{constant}. \tag{31}$$

Treating $Z = Z(T, p)$ and upon general differentiation, we have

$$dZ = (\partial Z/\partial T_g^0)_p \, dT_g^0 + (\partial Z/\partial p)_{T_g^0} dp = 0.$$

Therefore

$$dT_g^0/dp = -(\partial Z/\partial p)_{T_g^0}/(\partial Z/\partial T_g^0)_p. \tag{32}$$

Using the partition function of (24), in (32), we have

$$\frac{dT_g^0}{dp} = \frac{\sum_i \Delta V_i \exp[-\Delta G_i/RT]}{R\sum_i \frac{\Delta H_i}{RT} \exp[-\Delta G_i/RT]}. \tag{33}$$

In order to check the validity of the above expressions a knowledge of ΔV_i is essential. Unfortunately there is no simple way of even estimating these values. Since several of the required physical parameters are known (Rao *et al* 1973) for the case of ($40\,Ca(NO_3)_2$: $60\,KNO_3$) glass, we attempt the following examination of the consistency of the above expressions. K^+ ions are known to be dominent mobile species in $Ca(NO_3)_2$-KNO_3 glasses. The cage-vibrational frequency of K^+ ions in oxygen (NO_3 group) cage, is $\sim 200\ cm^{-1}$ or $\Delta E_1 \sim 500$ cals/mol. T_g of the above glass is 337 K. Hence $RT_g/\Delta E = (674/500)$. Using the thermal expansivity of the above glass as $1{\cdot}1 \times 10^{-4}\ deg^{-1}$ and molar volume as 41·3 cc. ΔV may be evaluated using (27) in a slightly approximated form: $\alpha(\text{conf})\ (\Delta V/VRT_g^2)\Sigma\Delta E_i f_i$ where it is assumed $\Delta V = \Delta V_1 = \Delta V_2 = \Delta V_3 \ldots = \Delta V_n$ and $\Delta H_i \simeq \Delta E_i$. The value of ΔV_i is thus found to be 0·50 cc. We may now use this value of ΔV_i in (33). With the same assumptions as above we find that the calculations yield (dT_g/dp) of 4·6 deg/kbar which is in fair agreement with the experimental value of 5·8 deg/kbar (compressibility may also be determined using $\Delta V_i = 0{\cdot}50$ cc. But the presence of ΔV_i as a square term in the expression renders it much less accurate. Indeed the value of bulk modulus turns out to be $2{\cdot}2 \times 10^{12}$ dynes/cm^2 as compared to the experimental value of $0{\cdot}16 \times 10^{12}$ dynes/cm^2 determined from sound velocity measurements (Rao *et al* 1973). For these approximate calculations the agreement is still noteworthy).

8. Transport properties from the model

Above the glass transition temperature, T_g^0, therefore, the particles are all essentially in the 'tissue' and particle excitations bring about configurational changes whose magnitude is large enough to manifest as a macroscopic flow. Configurational entropy of the system in this region can be directly related to the viscosity using Adam-Gibbs approach so that

$$\eta = \eta_0 \exp(B/TS_c),$$

where η_0 and B are constants of the viscosity expression, B being expressed in units of energy. S_c may be evaluated from a knowledge of heat capacities since $S_c = \int C_p(\text{conf})\, d\ln T$.

9. Model potential and its implications

A particularly simple potential scheme has been employed in these studies as discussed in §5.2 and schematically depicted in figure 3. An important implication of this

potential scheme is evident from (12) and (14). As particles are excited to higher vibrational states, their further exitations are governed by lower force constants and lower energies since exitations take place in regions of multiply connected potential wells. If the history of a single 'average' particle were to be traced as its motion 'evolves' from vibrational mode to translational mode through the glass transition, it absorbs quanta of energy from the thermal bath in stages, ΔE_1, $\Delta E_1/2$, $\Delta E_1/3$ . . . etc. $\Delta E_n/n$. Or with the effective force constants which keep 'softening' in steps of decreasing magnitude. Both Mossbauer and vibrational spectroscopic studies support such an energy scheme. In Mossbauer studies the Mossbauer intensity decreases during transition in a manner suggestive of a 'soft' mode (Ruby *et al* 1976; Flin *et al* 1976). In vibrational spectroscopy, the absorption band is seen to broaden towards low frequency side (Exarhos *et al* 1974) as temperature is increased. The energy level scheme in figure 3 can account for this effect. As higher levels get populated, their further excitations cause absorptions at lower energies and the inherent breadths of these bands produce an appearance of broadening towards low frequency side. It may be noted that since the ground state is still populated, the absorption at ΔE_1 continues to be present and the entire band is not shifted in the manner in which mode softening occurs in crystalline solids.

10. Concluding remarks

Glass transition model developed in this paper has taken full advantage of microheterogeniety. It has also assumed that microheterogeniety is a universal feature of glasses. This belief is gaining increasing acceptance in literature. The treatment of the model has been influenced greatly by a propensity to make it specifically relevent to simple ionic or metallic glasses. However, several aspects of the model are quite general. One of the important assumptions of the model relates to treating $f_0 N_t$ as a constant upto T_g^0. Apart from intuitive justification, this assumption is also somewhat justified by the final results obtained from the model. Perhaps one can dispense with this assumption and simply relate the decrease of cluster volume to the increase in tissue volume:

$$-\frac{dV_c}{dT} = \frac{1}{N_0}\frac{dN_t}{dT} = \frac{1}{N_0}\sum f_i N_0^0,$$

where N_0^0 is the number of particles in the ground state. Further, using the constraint $\Sigma N_0^i = N_t$ the behaviour of dV_c/dT may be formulated. Consequences of such treatment are being examined. The partition function used is rather heuristic. One can consider it as an *ad hoc* energy scheme without affecting any of our other conclusions. But using such a scheme provides meaningful interpretation of the physical phenomena involved in glass transition. As a result of the above assumptions the glass transition is shown to correspond to a constant value of Z (equation (31)). This is is a significant conclusion particularly if approached from high temperature liquid side. Glass transition seems to occur in supercooled liquids at a particular value of partition function. Also, this conclusion is independent of the detailed description of Z because at T_g^0, $Z = [a/(a-1)]$ and $a = V/V_c^0$ is a constant in the model.

The model developed here is in a large measure phenomenological, heuristic and semiquantitative. It is hoped that glass transition problem may be understood better if microheterogeniety is treated as an essential feature of all real glasses.

Acknowledgements

The author has benefitted immensely by the many discussions he had with Professor C N R Rao, on this subject. Prof. C N R's suggestions are gratefully acknowledged. Mr B Govinda Rao did the computations of both ξ and C_p. His help is acknowledged with thanks. The author also wishes to thank DST, India for research grants to investigate ionic glasses.

References

Adam G and Gibbs J H 1965 *J. Chem. Phys.* **43** 139
Angell C A and Moynihan C T 1969 *Molten salts* (ed.) G Mamantov (New York: Marcel Dekker)
Angell C A and Rao K J 1972 *J. Chem. Phys.* **57** 470
Angell C A and Sichina W 1976 *Ann. N.Y. Acad. Sci.* **279** 53
Boehm L, Ingram M D and Angell C A 1981 *J. Non. Cryst. Solids* **44** 305
Branda F, Buri A, Caferra D and Marotta L 1983 *J. Non Cryst. Solids* **54** 193
Bursill L A, Thomas J M and Rao K J 1981 *Nature (London)* **289** 157
Burton J J 1970 *J. Chem. Phys.* **52** 345
Burton J J 1973a *J. Chem. Phys.* **56** 3133
Burton J J 1973b *J. Chem. Soc. Faraday II* **69** 540
Button D P, Tandon R, King C, Veléz M H, Tuller H L and Uhlmann D R 1982 *J. Non Cryst. Solids* **49** 129
Cohen M H and Turnbull D 1959 *J. Chem. Phys.* **31** 1164
Cohen M H and Grest G S 1980 *Phys. Rev.* **B20** 1077
Cohen M H and Grest G S 1981 *Adv. Chem. Phys.* **48** 455
Exarhos G J, Miller P J and Risen Jr W H 1974 *J. Chem. Phys.* **60** 4145
Exarhos G J and Risen Jr W M 1971 *Chem. Phys. Lett.* **10** 484
Flinn P A, Zabransky B J and Ruby S L 1976 *J. Phys.* **C6 37** 739
Gaskell P H, Smith D J, Catto C J D and Cleaver J R A 1979 *Nature (London)* **281** 465
Gibbs J H and DiMarzio E A 1958 *J. Chem. Phys.* **28** 373
Gibbs J H 1963 *Modern aspects of vitreous state* (ed.) J D Mackenzie (London: Butterworths)
Goldstein M 1963 *J. Chem. Phys.* **39** 3369
Goldstein M 1969 *J. Chem. Phys.* **51** 3728
Goldstein M 1976a *J. Chem. Phys.* **64** 4767
Goldstein M 1976b *Phase transitions* (ed.) L E Cross (New York: Pergamon Press)
Goldstein M 1977 *J. Chem. Phys.* **67** 2246
Haddad J and Goldstein M 1978 *J. Non Cryst. Solids* **30** 1
Hemlata S, Parthasarathy G, Lakshmikumar S T and Rao K J 1983 *Philos. Mag.* **47** 291
Hoare M R 1976 *Ann. N.Y. Acad. Sci.* **279** 314
Hoare M R and Barker J 1976 *The structure of non crystalline materials* (ed.) P H Gaskell (London: Taylor and Francis)
Kauzmann W 1948 *Chem. Rev.* **43** 219
Kingery W D, Bowen H K and Uhlmann D R 1976 *Introduction to ceramics* (New York: John Wiley)
MacCall D W 1973 *J. Chem. Phys.* **47** 530
Moynihan C T, Macedo P B, Montrose C J, Gupta P K, DeBolt M A, Dill J F, Dom B E, Drake P W, Easteal A J, Elterman P B, Moeller R P, Sasabe H and Wilder J A, 1976 *Ann. N.Y. Acad. Sci.* **279** 15
Owen A E 1973 *Electronic and structural properties of amorphous semiconductors* (eds) P G Lecomber and J Mort (New York: Academic Press)
Parthasarathy R, Rao K J and Rao C N R 1981 *J. Phys. Chem.* **85** 3085
Parthasarathy R, Rao K J and Rao C N R 1984 *Chem. Soc. Rev.*
Phillips J C 1982 *Solid State Phys.* **37** 93
Rao C N R and Rao K J 1979 *Phase transitions in solids* (New York: McGraw Hill)
Rao K J 1979 *Bull. Mater. Sci.* **1** 181
Rao K J and Rao C N R 1982 *Mater. Res. Bull.* **17** 1337
Rao K J and Angell C A 1971 *Amorphous materials* (eds) R W Douglas and B E Ellis (New York: Wiley)
Rao K J, Helphrey D and Angell C A 1973 *Phys. Chem. Glasses* **14** 26

Rice S A 1975 *Topics in current chemistry* **60** 409
Rubinstein M 1976 *Phys. Rev.* **B14** 2778
Ruby S L, Zabransky B J and Flinn P A 1976 *J. Phys.* **C6 37** 745
Sakka S and Mackenzie J D 1971 *J. Non. Cryst. Solids* **6** 145
Schmidt V, Hopte J and Scholz R 1980 *Ultramicroscopy* **5** 223
Sundar H G K, Parthasarathy R and Rao K J 1982 **A37** 191
Turnbull D 1969 *Contemp. Phys.* **10** 473
Turnbull D and Cohen M H 1961 *J. Chem. Phys.* **34** 1120
Turnbull D and Cohen M H 1970 **52** 3038
Zarzycki J and Mezard R 1962 *Phys. Chem. Glasses* **3** 163